Application of phiLOV2.1 as a fluorescent marker for visualization of *Agrobacterium* effector protein translocation.

M.Reza Roushan, Milou A. M. de Zeeuw, Paul J.J. Hooykaas and G. Paul H. van Heusden*

Department of Molecular and Developmental Genetics, Institute of Biology Leiden, Faculty of Science, Leiden University, Sylviusweg 72, 2333 BE, Leiden, The Netherlands

*Corresponding author; G. Paul H. van Heusden

Running title:
phiLOV2.1 as a fluorescent marker for effector protein translocation

Keywords: *Agrobacterium*, phiLOV2.1 fluorescent protein, protein translocation, visualization, VirE2, effector proteins, *Nicotiana tabacum*, *Arabidopsis thaliana*, *Saccharomyces cerevisiae.*

E-mail addresses:
M.Reza Roushan: m.r.roushan@biology.leidenuniv.nl;
Milou A. M. de Zeeuw: milouannamaria@gmail.com;
Paul J.J. Hooykaas: P.J.J.Hooykaas@biology.leidenuniv.nl;
G. Paul H. van Heusden: g.p.h.van.heusden@biology.leidenuniv.nl;

Word count:
Total:6117. Summary: 212. Introduction:1256. Results:1718. Discussion:1365. References:1808.

SUMMARY

Agrobacterium tumefaciens can genetically transform plants by transferring a piece of single stranded DNA, called T-DNA, to its host. It uses a type IV secretion system (T4SS) to transfer the T-DNA, covalently bound to VirD2, along with several other effector proteins (VirE2, VirE3, VirD5 and VirF) into the host cells. However, the fate of the translocated proteins inside the host cell is only partly known. To further understand the translocation process and the function of the translocated effector proteins inside the host cell, several studies were conducted to visualize the translocated effector proteins. As GFP-tagged effector proteins are unable to pass the T4SS, other approaches like the split GFP system were used. Here, we investigated whether use can be made of the photostable variant of LOV, phiLOV2.1, to visualize effector protein translocation from *Agrobacterium* to yeast and plant cells. We were able to visualize the translocation of all five effector proteins investigated, both to yeast cells, to *Nicotiana tabacum* leaves and to *Arabidopsis thaliana* root explants that do not need to be transformed first to express GFP_{1-10}. Compared to the results obtained by using the split GFP system the signals were more condensed and more easily distinguishable from the background. On the other hand, fluorescence was weaker and more susceptible to photobleaching.

SIGNIFICANCE STATEMENT

Although *Agrobacterium tumefaciens* is widely used for genetic transformation of numerous different plant species, many aspects of the transformation process are still unclear. Here, we made use of the novel phiLOV2.1 fluorescent protein to directly visualize effector protein translocation to host cells. In contrast to previous GFP based methodologies, the new method does not rely on special transgenic host cells, thus we successfully visualized proteins translocation into *Arabidopsis thaliana* root, tobacco leaf and yeast cells.

INTRODUCTION

Over 640 dicotyledonous plant species are susceptible to infection by *Agrobacterium tumefaciens* resulting in the formation of crown gall tumors (De Cleene and De Ley, 1976; Nester *et al* ., 1984). During the infection a piece of single-stranded DNA, called T-DNA, is translocated to the nucleus of host cells where it is integrated into the genome (Tinland *et al* ., 1994). The genes that are involved in virulence and T-strand formation are located on a tumor inducing (Ti) plasmid (Larebeke *et al* ., 1974; Nester *et al.*, 1975). The *virulence* (*vir*) region on this plasmid consists of several operons: *virA*-*R* (Stachel and Nester, 1986; Zhu *et al*., 2000). Wounded plant cells excrete several compounds, including phenolic compounds and sugars. These compounds activate VirA and VirG, resulting in expression of the other *vir* genes (Lee *et al* ., 1996). It has been shown that the effector proteins VirD2, VirD5, VirE2, VirE3 and VirF translocate into the host cell through a type 4 secretion system (T4SS) formed by VirB1 to 11 and VirD4 (Christie *et al* ., 2005). This translocation is mediated by C-terminal signal sequences and can occur independently of T-DNA transfer (Vergunst et al., 2000; Vergunst et al., 2005). As VirD2 becomes covalently linked to the 5' end of the T-DNA when acting as a relaxase, it can mediate transport of the T-DNA into host cells (Albright *et al.*, 1987)(Howard *et al .,* 1992; Pansegrau *et al .* 1993). However, even in absence of T-DNA, VirD2 can be transported through the T4SS (Vergunst *et al* ., 2005). VirD2 contains one bipartite nuclear localization signal (NLS) located at the C-terminal part and one monopartite NLS at the N-terminal part, that may guide the T-DNA to the nucleus of the host cell (Herrera-Estrella *et al*., 1990; Howard *et al*., 1992; Tinland *et al*., 1992; Rossi *et al*., 1993; Citovsky *et al*., 1994; Mysore *et al*., 1998; Shurvinton *et al*., 1992; Vogel and Das, 1992). VirE2 binds cooperatively to single-stranded DNA without any sequence specificity (Gietl *et al* ., 1987). Inside the host cell, the T-DNA may be coated by VirE2 proteins, thereby possibly protecting the T-DNA against host nucleases (Citovsky *et al .,* 1989; Rossi *et al*., 1996). VirE2 has two potential NLSs, but compared to the single NLS of VirD2 their activity is weaker and it may be hidden when the protein is bound to the T-strand (Citovsky *et al* ., 1992). Whether these NLSs are involved in nuclear import of VirE2 is still unclear. Ziemienowicz *et al.* (2001) suggested that VirD2 is essential and sufficient

for import of short single-stranded DNA into the plant nucleus, whereas for import of longer DNA VirE2 is also required. Furthermore, localization of VirE2 in the nucleus of tobacco cells has been reported (Tzfira *et al* ., 2001). On the other hand, Djamei *et al*. (2007) were unable to obtain evidence that VirE2 by itself is imported into the nucleus of *Arabidopsis thaliana* cells. Instead, the VirE2 Interacting Protein 1 (VIP1) may guide VirE2 and the associated T-complex into the nucleus. VIP1 may also be important for the association of the T-complex with the host chromatin (Tzfira *et al* ., 2001) However, recently the role of VIP1 in the transformation process was questioned (Shi *et al* ., 2014). The virulence protein VirF is a host range factor of *Agrobacterium* (Hooykaas *et al*., 1984; Melchers *et al .,* 1990). This protein contains an F-box domain, and may form a Skp-Cullin-F-box protein (SCF) complex by interacting with the plant proteins ASK1 and ASK2 (Schrammeijer *et al* ., 2001; Magori and Citovsky, 2011). This complex may enable T-DNA integration by proteasomal degradation of VIP1 and VirE2 (Tzfira *et al* ., 2004). In addition, it may destabilize VFP4, a transcriptional activator of defense response genes (García-Cano et al , 2017). VBF, a plant F-box protein, might functionally replace VirF in plant species that do not require VirF for successful transformation (Zaltsman *et al* ., 2010). VBF can interact with VIP1 and VirE2, thereby eliciting the degradation of these proteins (Wang *et al* ., 2014). VirE3 interacts with pBrp, a plant-specific transcription factor (García-Rodríguez *et al* ., 2006). pBrp localizes at the outside of plastids; however, when the cell is stressed or when VirE3 is present, pBrp translocates to the nucleus to stimulate transcription. Niu *et al .* (2015) showed that VirE3 activates the *VBF* promoter and thus possibly indirectly regulates the levels of VirE2 and VIP1. This clarifies why the transformation is only slightly decreased with a mutation in either *virF* or *virE3*, while the inactivation of both genes leads to low transformation efficiency (García-Rodríguez *et al* ., 2006). VirD5 has two bipartite NLSs, but is not essential for tumor formation. Wang *et al .* (2014) demonstrated that VirD5 can interact directly with the VIP1. They showed that VirD5 competes with VBF to bind to the VIP1-VirE2 complex, thereby inhibiting the degradation of this complex. In addition, VirD5 interacts with another VirE2 binding protein, VIP2 (Wang et al , 2018). On the other hand, Zhang *et al .* (2017) showed that VirD5 can inhibit plant growth by provoking

chromosome mis-segregation during mitosis. After ectopic expression in yeast GFP-VirD5 was localized in dot-shaped structures inside the nucleus.

To further understand the role of the translocated effector proteins in the transformation process several studies aimed to visualize protein translocation into the host cell. Such studies are hampered by the inability of GFP-tagged proteins to translocate through the T4SS probably due to the rigidness of the GFP protein. Translocation of the *Agrobacterium* effector proteins was successfully visualized by using the split GFP technique (van Engelenburg and Palmer, 2010;Sakalis, 2013; Sakalis *et al*., 2014; Li *et al .,* 2014; Yang *et al* ., 2017; Li and Pan., 2017). *Saccharomyces cerevisiae* and plants expressing the first ten helices of GFP (GFP_{1-10}) were infected with *Agrobacterium* strains expressing the effector proteins tagged with the remaining helix of GFP (GFP_{11}). After translocation of the GFP_{11}-tagged effector protein into the host cell, GFP is reconstituted and the translocated protein can be visualized. GFP_{11}-VirE2 formed dot-shaped and filamentous structures of different lengths after translocation to yeast and plant cells (Sakalis *et al.,* 2014; Li *et al*., 2014; Yang *et al* ., 2017; Li and Pan, 2017). The split GFP technique has some drawbacks. For this technique a genetically modified host expressing GFP_{1-10}, is needed. Another disadvantage is that translocated proteins will only be visible in those cellular compartments where also GFP_{1-10} is available (Park *et al* ., 2017). Recently, protein translocation into mammalian cells through the type 3 secretion system of *Shigella flexneri* was visualized using phiLOV2.1, an improved version of LOV (Gawthorne *et al .,* 2016). LOV, a plant fluorescent flavoprotein, is a member of the family of blue-light receptor kinases called phototropins, regulated either by **L**ight, **O**xygen or **V**oltage (Huala *et al* ., 1997; Buckley *et al .,* 2015). Compared to LOV phiLOV2.1 has increased fluorescence and photostability (Christie *et al* ., 2012a, b). phiLOV2.1 is much smaller than GFP, 12.1 kDa *vs*. 27 kDa, which may be an advantage in studies on protein translocation.

In this study, we used phiLOV2.1 to tag virulence proteins VirD2, VirD5, VirE2, VirE3 and VirF to visualize their translocation and localization in cells of the yeast *S. cerevisiae*, in *Nicotiana tabacum* leaves and in *A, thaliana* roots. We successfully

visualized the expression of phiLOV2.1-tagged virulence proteins in *Agrobacterium* and their translocation into the host cells. On the other hand, compared to the split GFP system, using phiLOV2.1 results in a weaker fluorescent signal and higher photobleaching.

RESULTS

Ectopic expression of phiLOV2.1-tagged virulence proteins in yeast.

First we investigated whether *Agrobacterium* effector proteins can be visualized by confocal microscopy when tagged with phiLOV2.1. To this end, we ectopically expressed N-terminally phiLOV2.1-tagged effector proteins in yeast under control of the *MET17* (alias *MET25*) promoter. In addition, a plasmid was constructed expressing VirE2 internally tagged with phiLOV2.1 at proline-39 (39phiLOV2.1-VirE2). Tagging with GFP_{11} or insertion of a peptide at this position was shown not to affect the biological activity of VirE2 (Zhou and Christie, 1999; Li et al , 2014). As shown in Figure 1 (A-F) a fluorescent signal was found for all five phiLOV2.1-tagged effector proteins. To study whether the subcellular localization of the phiLOV2.1-tagged effector proteins is similar to that found using other fluorescent tags, we expressed GFP_{11}-tagged effector proteins in a yeast strain expressing GFP_{1-10}. This resulted in a fluorescent signal, except for GFP_{11}-tagged VirE3 and VirF (Figure 1, G-K). The localizations of the effector proteins observed after using the different tags are highly similar for most effector proteins. We observed filamentous structures and dots inside cells expressing either internally or N-terminally tagged phiLOV2.1-VirE2 and also in cells expressing VirE2 internally-tagged with GFP_{11} (Figure 1A, B and G). In contrast, only sporadically a dot-like structure was found in cells expressing N-terminally tagged GFP_{11}-VirE2 (Figure 1H), similarly as we reported previously (Sakalis *et al* ., 2014). VirD2 and VirD5 were found concentrated in the nucleus, independently of the tag used (Figure 1, C, E, I, K). This nuclear localization was confirmed by 4',6-diamidino-2-phenylindole (DAPI) staining (Figure S1). phiLOV2.1-VirF was observed all over the yeast cell (Figure 1D) whereas we were not able to obtain reliable signals after expression of GFP_{11}-VirF. Dot-like structures, located inside the nucleus, were found in cells expressing phiLOV2.1-VirE3 (Figure 1F). Also this

nuclear localization was confirmed by DAPI staining (Figure S1). No fluorescence could be detected after expression of GFP_{11}-VirE3. Expression of free phiLOV2.1 in yeast resulted in a fluorescent signal all over the yeast cell (supplementary Figure S2A), indicating that phiLOV2.1 itself is not targeted to a specific cellular location.

Expression of phiLOV2.1-tagged virulence proteins in *Agrobacterium*

To study the expression of virulence proteins in *Agrobacterium* and their translocation to yeast and plant cells, we created phiLOV2.1 fusions in the pBBR6 plasmid backbone under control of the endogenous promoters. These constructs were introduced in *Agrobacterium* strains lacking the corresponding endogenous *vir* gene. The expression of the *vir* genes was induced by addition of acetosyringone to a final concentration 200µM. After 6 and 24 hrs expression was analyzed by fluorescence microscopy. As shown in figure 2 in the *Agrobacterium* strains LBA2572(pBBR6-39phiLOV2.1-VirE2)(containing T-DNA) and LBA2573(pBBR6-39phiLOV2.1-VirE2)(T-DNA deficient) after 6 hrs expression of 39phiLOV2.1-VirE2 was observed in more than 50% of *Agrobacterium* cells independently of the presence of T-DNA. After 24 hrs the phiLOV2.1 signal in the *Agrobacterium* strain lacking T-DNA was spread over the entire cell with somewhat increased intensity at the poles. Interestingly, the expression of 39phiLOV2.1-VirE2 was much higher in cells containing T-DNA and it was localized near the membrane as horseshoe-like structures in approx. 80% of the cells (Figure 2D). Very low fluorescent signals were found for the other phiLOV2.1-tagged virulence proteins, too low to draw conclusions.

Biological activity of phiLOV2.1-tagged virulence proteins

To investigate whether the virulence proteins have retained their activity after tagging with phiLOV2.1 we performed tumor formation assays. To this end, *N. glauca* shoots were injected with the different *Agrobacterium* strains and after 4 weeks tumor formation was scored. Tumors were easily visible after injection of the positive control strain LBA1010 and no tumors were found after injection of the control strain lacking T-DNA

(LBA1100) (Figure S3 A and B, respectively). After injection of LBA2569 which lacks *virD*2, no tumors were found, in agreement with the essential role of VirD2 in *Agrobacterium*-mediated transformation (AMT) (Figure S3C). Injection of LBA2569 (phiLOV2.1-VirD2) expressing phiLOV2.1-VirD2, resulted in small tumors, indicating that phiLOV2.1-VirD2 is at least partially functional (Figure S3D). Injection of LBA2572 lacking virE2 or LBA2572(phiLOV2.1-VirE2) expressing N-terminally tagged phiLOV2.1-VirE2, did not result in tumor formation, indicating the essentiality of VirE2 for tumor formation on *N. glauca* and that N-terminal tagging of VirE2 results in loss of activity (Figure S3 E and F). In contrast, injection of LBA2572(39phiLOV2.1-VirE2) which expresses 39phiLOV2.1-VirE2 results in tumor formation, although the tumors are smaller in size. This indicates that VirE2 can be tagged internally with phiLOV2.1 at proline-39 without complete loss of function (Figure S3G). Injection of LBA2572(39GFP_{11}-VirE2) resulted in larger tumors than injection of LBA2572(39phiLOV2.1-VirE2) indicating that tagging with GFP_{11} has less effect than tagging with phiLOV2.1 on the activity of VirE2 (Figure S3H). As VirD5, VirE3 and VirF are not essential for tumor formation on *N. glauca*, the activity of the phiLOV2.1-tagged versions of these proteins could not easily be tested. García-Rodríguez *et al* . (2006) showed that deletion of both *virE3* and *virF* resulted in a decreased tumor size. As shown in Figure S3I, the *virE3 virF* double mutant LBA2566 generates small sized tumors, while strains complemented with phiLOV2.1-VirF were able to generate somewhat larger tumors than the uncompleted double mutant (Figure S3J). The effect of complementation by phiLOV2.1-VirE3 is less clear (Figure S3K).

Visualization of translocation of phiLOV2.1- or GFP_{11}-tagged effector proteins into yeast after AMT.

To investigate translocation of effector proteins into yeast during AMT we used *Agrobacterium* strains expressing phiLOV2.1- and GFP_{11}-tagged effector proteins. *Agrobacterium* strains expressing phiLOV2.1-tagged effector proteins were co-cultivated for 24-48 hrs with BY4741 and clear fluorescent signals were observed inside the yeast cells for all five Vir proteins (Figure 3 A-F). The strains expressing the GFP_{11}-tagged

proteins were co-cultivated with a yeast strain expressing GFP_{1-10}. As shown in Figure 3 G-K, a clear fluorescent signal was observed in the yeast cells after co-cultivation for 42 hrs with *Agrobacterium* strains expressing GFP_{11}-tagged VirE2, -VirD2 and -VirD5. The number of yeast cells containing the translocated proteins is rather low, less than one percent for all virulence proteins and independently of the tag used. For most virulence proteins dot–shapes fluorescent structures were observed, irrespective of the tag used. Because of the low amounts of proteins translocated into the yeast cell, it was difficult to perform additional staining to identify subcellular organelles. Using the same microscope setting as used above no fluorescent signal could be detected in the yeast cells after co-cultivation with an *Agrobacterium* strain lacking phiLOV2.1 (supplementary Figure S2B). Agrobacteria recovered from the co-cultivation mixture have hardly detectable phiLOV2.1-fluorescence.

Translocation of phiLOV2.1-tagged effector proteins from *Agrobacterium* to *A. thaliana* roots

To analyze 39phiLOV2.1-VirE2 translocation to plant tissue, *A. thaliana* root explants were co-cultivated with *Agrobacterium* strain LBA2573(39phiLOV2.1-VirE2) for 15 hrs. Confocal microscopy revealed many fluorescent dot-shaped structures inside the root cells (supplementary Figure S4). Some of these dots were found colocalized with structures resembling the nucleus. To further investigate the possible nuclear localization of the translocated VirE2, the co-cultivation was repeated using *A. thaliana* Col-0 (NLS-RFP) root explants expressing nuclear RFP. Confocal microscopy revealed fluorescent dot-shaped structures and some of them co-localizing with the nuclear marker. An example is shown in Figure 4A. On the other hand, in the majority of cells 39phiLOV2.1-VirE2 is present in dot-shaped structures elsewhere in the cell.

To analyze the translocation of the other effector proteins, *A. thaliana* Col-0 (NLS-RFP) root explants were co-cultivated with *Agrobacterium* strains LBA2569(pBBR6-phiLOV2.1-VirD2), LBA3550(pBBR6-phiLOV2.1-VirD5) and LBA2560(pBBR6-phiLOV2.1-VirF). As shown in figure 4, translocation of these effector proteins was detected. Nuclear localization of translocated VirD2 and VirD5 was observed after co-cultivation for 42 hrs (Figure 4B and C).Translocated VirF did not colocalize with the

nuclear marker, but only few phiLOV2.1-VirF translocation events could be found. After co-cultivation with LBA1010 lacking any phiLOV2.1 protein, as expected, no phiLOV2.1 fluorescence could be detected (supplementary Figure S5A). As mentioned above, Agrobacteria recovered from the co-cultivation mixture, have very low levels of the phiLOV2.1-tagged effector proteins. Therefore, it is very unlikely that the fluorescent signals are caused by uptake of Agrobacteria rather than by protein translocation. In line with this conclusion, we showed that after co-cultivation of *A. thaliana* roots with *Agrobacterium* strain LBA3567(placZ-GFP) constitutively expressing GFP, no GFP fluorescence inside cells could be found, even after inspection of more than 20 root explants in two separate experiments. Instead, only *Agrobacterium* attached to the outside of the roots was observed (supplementary Figure S5B).

Translocation of phiLOV2.1-tagged effector proteins from *Agrobacterium* to *N. tabacum* SR1 leaves

In previous studies the split GFP approach has been used to visualize VirE2 translocation from *A. tumefaciens* into *N. benthamiana* and *N. tabacum* leaf tissues (Sakalis *et al* 2014; Li *et al* , 2014;Li and Pan, 2017). Translocated VirE2 was mostly found in dot-shaped and filamentous structures. Li and Pan (2017) showed data which suggested that in *N. benthamiana Agrobacterium*-delivered GFP_{11}-VirE2 initially accumulated on plant cytoplasmic membranes that subsequently were internalized through clathrin-mediated endocytosis to form endomembrane compartments. To investigate translocation of 39phiLOV2.1-VirE2 four weeks old *N. tabacum* SR1 leaves were infiltrated with *Agrobacterium* strains LBA2572 (containing T-DNA) or LBA2573 (lacking T-DNA) harboring pBBR6-39phiLOV2.1-ViE2. After 21 hrs filamentous and dot-like structures of VirE2 were found in the cytoplasm and near the plasma membrane of leaf epidermal cells (Figure 5 A-B and C-D, respectively). After infiltration of *N. tabacum* SR1 with *Agrobacterium* strains LBA2564(pBBR6-phiLOV2.1-VirE3), LBA2569(pBBR6-phiLOV2.1-VirD2), LBA2560(3163GFP_{11}-F) or LBA253551(pBBR6-phiLOV2.1-VirD5), similar accumulations near the plasma membrane (possibly the endomembrane) were observed for phiLOV2.1-tagged VirE3, VirD2, VirF and virD5 (Figure 6).

VirE2 interactions with microtubules in yeast and *A. thaliana* protoplasts

Salman *et al .* (2005) showed that VirE2 can bind *in vitro* to microtubules. In addition, we obtained evidence that filaments formed by VirE2 in yeast cells are associated with the microtubules (Sakalis *et al* , 2014). As shown in figure 1B ectopic expression of 39-phiLOV2.1-VirE2 in yeast resulted in the formation of fluorescent filamentous structures. To investigate the effect of tubulin disruption on these filamentous structures we expressed 39phiLOV2.1-VirE2 and disrupted the microtubules by benomyl treatment. As shown in Figure 7 (upper panel) this treatment resulted in disruption of the VirE2 filaments. To investigate the effect of tubulin disruption on VirE2 filaments in a plant background, we expressed 39phiLOV2.1-VirE2 in *A. thaliana* protoplasts and disrupted the microtubulins by oryzalin treatment. As shown in figure 7 (lower panel) in protoplasts 39phiLOV2.1-VirE2 formed dot-shaped structures and these structures are more closely to the cell membrane upon treatment with oryzalin.

DISCUSSION

Effector protein translocation is essential for the trans-kingdom transfer of T-DNA from *Agrobacterium* into eukaryotic host cells. Despite its importance many aspects of the translocation process and the fate of the translocated proteins in the host cell are still not yet clarified. Visualization *in vivo* may provide more detailed information on the translocation process. GFP-tagging of effector proteins was not successful, because of the inability of GFP-tagged proteins to translocate through the T4SS, probably due to the rigidness of the GFP protein. On the other hand, we applied successfully Bimolecular Fluorescence Complementation (BiFC) to visualize translocation of VirE2 into yeast cells (Sakalis *et al*., 2014). To this end, yeast cells expressing VirE2 tagged with one half of the YFP analog Venus were co-cultivated with *Agrobacterium* expressing VirE2 tagged with the remaining half of Venus. As VirE2 binds to itself, protein translocation brings the two parts of Venus close together, resulting in a fluorescent protein. Alternatively, the split GFP system (Van Engelenburg and Palmer, 2010) has been used. Yeast and

plants expressing the first ten helices of GFP (GFP_{1-10}) were infected with *Agrobacterium* strains expressing the effector proteins tagged with the remaining helix of GFP (GFP_{11}). After translocation of the GFP_{11}-tagged effector protein into the host cell, GFP is reconstituted and the translocated protein can be visualized. With this approach translocation of VirE2 was visualized (Sakalis *et al.,* 2014; Li *et al* , 2014; Yang *et al* ., 2017; Li and Pan, 2017). On the other hand, the split GFP technique also has its shortcomings. It may require several hours before GFP_{1-10} is matured and reconstituted with GFP_{11} (Van Engelenburg and Palmer, 2010). Furthermore, a genetically modified host expressing GFP_{1-10}, is needed. Another disadvantage is that the translocated proteins will only be visible in those cellular compartments where also GFP_{1-10} is available (Park *et al* , 2017). Therefore, in this study we explored whether the LOV-derived fluorophore phiLOV2.1 can be employed to study protein translocation from *Agrobacterium* to yeast and plant cells. The key advantages of using phiLOV2.1 as a reporter are its stability over a wide range of pH values, its molecular oxygen independency and its small size (12.1 kDa). On the other hand, photo bleaching and weaker signals in plant cells are disadvantages (Buckley *et al* , 2015). Recently, protein translocation into mammalian cells through the type 3 secretion system of *Shigella flexneri* was successfully visualized using phiLOV2.1 (Gawthorne *et al* . 2016).

Translocation of VirE2 has been studied before by using the BiFC and split GFP approaches (Sakalis *et al.* 2013, 2014); Li *et al* , 2014; Yang *et al* ., 2017; Li and Pan, 2017). Translocated VirE2 was found in dot-shaped and filamentous structures in both yeast cells as well as in *N. tabacum* and *N. benthamiana* leaves. In this study, translocated 39phiLOV2.1-VirE2 was found in similar dot-shaped and filamentous structures inside *N. tabacum* leaf cells (Figures 5 and 6). In yeast and *A. thaliana* root cells translocated 39phiLOV2.1-VirE2 was mainly present in dot-shaped structures (Figures 3 and S4, respectively). Compared to GFP_{11}-tagged VirE2 phiLOV2.1-tagged VirE2 gave more condensed signals which are better distinguishable from the background. Interestingly, in 5 out of 37 of *A. thaliana* root cells which showed phiLOv2.1-VirE2 signals, we found translocated 39phiLOV2.1-VirE2 colocalizing with the nuclear marker, suggesting that it may have entered the nucleus (Figure 5A). Li *et al* observed trafficking of GFP_{11}-tagged VirE2 inside plant cells but not in yeast (Li et al ,

2014). We were able to observe similar movement of 39GFP$_{11}$-VirE2 translocated to *N. tabacum* cells (Movie S1). Our attempts to record movement of translocated 39phiLOV2.1-VirE2 in plant cells were unsuccessful mainly because of the fast bleaching of the phiLOV2.1 fluorescence. Previously, we showed that ectopically expressed GFP/YFP/CFP-tagged VirE2 formed filamentous structures associated with the microtubules in both yeast and *A. thaliana* protoplasts (Sakalis *et al* , 2014). Similar filamentous structures were found in the present study for ectopically expressed 39phiLOV2.1-VirE2 (Figures 1 and 7).These structures were strongly affected by treatments to disrupt microtubules (Figure 7).

VirD2 contains nuclear localization signals that guide the T-complex to the nucleus of the host cell (Herrera-Estrella *et al*., 1990; Howard *et al*., 1992; Tinland *et al*., 1992; Rossi *et al*., 1993; Citovsky *et al*., 1994; Mysore *et al*., 1998; Shurvinton *et al*., 1992; Vogel and Das, 1992). Ectopically expressed GFP-VirD2 has a nuclear localization in both yeast and plant cells (Citovsky *et al*., 1994; Wolterink-van Loo *et al* ., 2015). In this study we found a similar localization for both GFP$_{11}$- and phiLOV2.1-tagged VirD2 ectopically expressed in yeast (Figures 1 and S1). VirD2 translocation form *Agrobacterium* to yeast could be shown for both GFP$_{11}$- and phiLOV2.1-tagged VirD2. The translocated VirD2 is most likely located in the nucleus, but because of the low amount of translocated VirD2 we were unable to determine the exact subcellular localization. phiLOV2.1-VirD2 translocated to *A. thaliana* root cells was found in the nucleus (Figure 4), whereas in *N. tabacum* leaves it was found in dot-shaped structures some of them close to the cell membrane (Figures 6 and 7).

Translocation of the other effector proteins, i.e. VirE3, VirD5 and VirF, has not been extensively studied before. VirE3-RFP expressed in *A. thaliana* protoplasts has a nuclear localization (Niu et al 2015). As shown in Figure 3 and S1, in yeast translocated phiLOV2.1-VirE3 localizes in dot-shaped structures, inside the nucleus. In *A. thaliana* roots translocated phiLOV2.1-VirE3 also localizes in dot-shaped structures, some of them close to the cell membrane (Figure 6). Recently, Zhang *et al* showed ectopically expressed GFP-VirD5 was clustered in bright dots in the nucleus (Zhang *et al* , 2017). Translocated phLOV2.1-VirD5 was found both inside and outside the nucleus in *A.*

thaliana root cells (Figure 4). Reconstituted GFP signals were not detected in yeast cells expressing GFP_{11}-tagged VirE3 and VirF, possibly due to inaccessibility of the GFP_{11}-tag for GFP_{1-10}. Translocation of phiLOV2.1-VirE3 and of phiLOV2.1-VirF from *Agrobacterium* to both yeast and plant cells could be shown (Figures 3, 4 and 6). However, its subcellular location is still unclear and is dependent on the host cells used.

Li and Pan. (2017) showed that *Agrobacterium* VirE2 delivery into host cells was facilitated by the clathrin endocytosis pathway mediated by interaction of dileucine motifs of VirE2 with the AP2M clathrin adaptor. Initially, translocated VirE2 was at the plasma membrane and subsequently entered the cell by trapping inside endocytosis vesicles. We observed a similar localization near the plasma membrane not only for VirE2 (Figure 5 C and D) but also for VirD2, VirF, VirD5 and VirE3 (Figure 6). Analysis of the amino acid sequences of these effector proteins based on putative endocytic motifs identified by the Eukaryotic Linear Motif resource for functional sites in proteins (www.elm.eu.org) revealed the presence of tyrosine-based, dileucine and DPF/W motifs in VirD2, VirF, VirE2 and VirE3 which may interact with the AP adaptor (supplemental Figure S6). Therefore, these proteins may enter the host cell by the endocytosis pathway as well. However, further studies are required to establish whether the clathrin-mediated endocytosis pathway is indeed involved in the uptake of VirD2, VirE3, VirD5 and VirF.

In summary, we can conclude from this study that phiLOV2.1 can successfully be used to study protein translocation from *Agrobacterium* to yeast and plant cells. A great advantage over the split GFP approach is that expression of GFP_{1-10} in the host is not needed. Furthermore, compared to GFP_{11}-tagged VirE2 phiLOV2.1-tagged VirE2 gave more condensed signals which are better distinguishable from the background. On the other hand fluorescence signals are weaker. Despite we used the improved phiLOV2.1 form of LOV, photobleaching is still considerable. Remarkably, phiLOV2.1-tagged effector proteins were hard to detect inside *Agrobacterium*. Most of the translocated effector proteins were found in dot-shaped and filamentous structures. It remains to be established whether the effector proteins are functional while in such structures. It is expected that host cells respond to the presence of unwanted proteins by degradation or transport to sites where these are shielded from the rest of the cell. So, it is possible that

the majority of the translocated proteins are not involved in the transformation process and only a minor fraction can escape the degradation process and can fulfill their role in the transformation process.

EXPERIMENTAL PROCEDURES

Yeast strains and media. Yeast strains used in this study are listed in Table S1. All yeast strains were grown in YPD medium or selective MY medium supplemented, if required, with histidine, tryptophan, methionine and/or uracil to the final concentration of 20 mg/ml (Zonneveld, 1986). Yeast transformation was performed using the Lithium Acetate method (Gietz *et al* ., 1995). Yeast strains carrying plasmids were obtained by transforming parental strains with the appropriate plasmids followed by selection for histidine and/or uracil prototrophy.

***Agrobacterium* strains and media.** The *Agrobacterium* strains used are listed in Table S2. *Agrobacterium* was grown in LC supplemented with the appropriate antibiotics (40 µg/ml gentamycin, 20 µg/ml rifampicin) at 28˚C and 175 rpm. *Agrobacterium* strains carrying plasmids were obtained by electroporation as described by Den Dulk-Ras and Hooykaas, (1995).

Plant lines. The plant lines used in this study were: *Nicotiana tabacum* (SR1), *N. tabacum* (SR1) expressing GFP_{1-10} (Sakalis *et al* ., 2014), *Nicotiana glauca*, *A. thaliana* Columbia-0 (Col-0) and *A. thaliana* Col-0 mRFP-NLS (At2051) (obtained from Prof. Dr. S. B. Gelvin , Purdue University).

Agroinfiltration. *N. tabacum* was grown on soil at 25°C, 50% relative humidity and 16 hrs photoperiod, to full plants and after one month young leaves were selected for agroinfiltration. After overnight growth of *Agrobacterium* strains at 28°C in LC medium, cultures were resuspended to the OD_{600}≈0.8 in 10 ml of induction medium with 200 µM acetosyringone (AS) and incubated for three hours at 28°C. The lower surface of the leaves of one-month-old *N. tabacum* SR1 was injected with this culture with a blunt-

tipped 10 ml syringe using gentle pressure. After 10-48 hours the lower side of the leaves was analyzed using confocal microscopy.

Tumor formation assay. To assess whether the tagged virulence proteins are still biologically active, a tumor formation assay was performed. The plasmids with the genes for the tagged effector proteins were introduced in *Agrobacterium* strains with a deletion for that particular *vir* gene. An overnight culture of *Agrobacterium* was washed and resuspended with 0.9% (w/v) NaCl solution to an OD_{600} of 1.0. After growing the *N. glauca* plants for six to seven weeks at 25°C, 75% relative humidity and 16 hours photoperiod, their stem was damaged with a sterile toothpick, followed by the inoculation of 20 µl of the *Agrobacterium* culture. After four weeks the tumor formation was scored and photographed.

Root protein translocation assay. *A. thaliana* Col-0 wild type and *A. thaliana* Col-0 mRFP-NLS (At2051) were used for the root protein translocation assays. Approximately 3 mg of sterilized seeds were grown in 50 ml of B5 medium while shaking 90 rpm at 21°C with 16 hours of light per day and 50% relative humidity. After at least eight days the roots were separated from the hypocotyls and placed on callus induction medium (CIM) for three days. Subsequently, the roots were placed in a clean sterile petri dish containing 20 ml of the *Agrobacterium* overnight culture with a OD_{600} of 0.3 and incubated for at least 20 min at room temperature. The roots were then dried on a sterile paper towel and placed on CIM containing 100 µM acetosyringone. The cocultivation plates were placed underneath a piece of aluminum foil in the growth chamber with a temperature of 24°C and 50% relative humidity. After 20 to 48 hrs, root protein translocation was analyzed using confocal laser scanning microscopy. LBA1010 was used as a negative control. B5 and CIM are described by Vergunst *et al.*(1998) as liquid growth medium (LGM) and callus induction medium (CIM), respectively.

Protoplast transformation. Protoplasts were derived from a five days old *A. thaliana* Col-0 cell suspension as described by Schirawski *et al*. (2000). and were transformed with 10 µg of plasmid DNA per 10^6 protoplasts using Polyethyleneglycol (PEG) (Schirawski *et al* ., 2000). The transformed protoplasts were incubated at 27°C in the dark for 24 hours before treatments and microscopy.

Microscopic analysis. The localization of phiLOV2.1 fused to the Vir proteins expressed in yeast and plants was analyzed using the Zeiss Imager M1 equipped with a LSM5 Exciter, using a 40x (aperture 1.30) or a 63x (aperture 1.40) magnifying objectives. The phiLOV2.1 signal was detected using an argon laser of 488 nm and a band-pass emission filter of 505-600 nm. The nuclear marker NLS::RFP was captured with an excitation wavelength of 543 nm and a 650 nm long-pass emission filter. Microscopy of *Agrobacterium* expressing phiLOV2.1-tagged effector proteins was done with an Axioplan2 imaging microscope equipped with DIC and fluorescent filters to detect phiLOV2.1 signals at excitation wavelength of 488 and emission of 505-600 nm. The ImageJ (Abràmoff *et al* ., 2004) software was used to process and analyze the pictures.

Plasmid constructions. All plasmids used and constructed in this study are listed in Table S3. *E. coli* strain XL1-Blue was used for cloning of the plasmids and the cultures were grown in LC medium containing 10 µg/ml gentamycin or 100 µg/ml carbenicillin while shaking 175 rpm at 37˚C. PCR amplifications were done with Phusion™ High-Fidelity DNA Polymerase. Table S4 lists all primers used for PCR amplification and sequencing.

DNA fragments with phiLOV2.1 including or lacking its stop codon, were amplified by PCR on pGEX-6p1[phiLOV2.1] using primer pairs *XbaI*-phiLOV2.1-Fw and *BamHI*-phiLOV2.1-Rev or *XbaI*-phiLOv2.1-Fw and *BamHI*-phiLOv2.1ΔTAA-Rev, respectively. Then, they were used to replace GFP in pUG36 after digesting with *XbaI* and *BamHI*, yielding pUG36phiLOV2.1 and pUG36phiLOV2.1ΔTAA, respectively.

Li et al , 2014 showed that VirE2 (from *Agrobacterium* strain EHA105) can be tagged internally at proline-54 with GFP_{11} without loss of function, as originally found by (Zhou and Christie, 1999). The corresponding site in VirE2 from the octopine Ti-plasmid used in our studies, is proline-39. To insert GFP_{11} at this position, a DNA fragment was synthesized containing the 5' -end of *virE2* and GFP_{11} adjacent to the codon for proline-39, with *Spe*I and *Bgl*II restriction sites at the ends by Eurofins (Germany):

5’- ACTAGT*CATATG*GATCTTTCTGGCAATGAGAAATCCAGGCCTTGGAAGAAGGCG
AATGTCAGTTCCAGCACCATCTCCGATATTCAGATGACGAATGGCGAAAACCTTGA
ATCAGGGAGC**CCT**CGGGACCACATGGTGCTGCACGAGTACGTGAACGCCGCCGG
CATCACAACCCGAACGGAAGTTTTAAGCCCACGTCTGGATGATGGATCGGTCGATT
CCTCCTCCAGCCTTTATTCTGGCAGCGAGCACGGAAATCAAGCTGAGATTCAAAAA
GAGCTGTCCGCCTTGTTCTCGAACATGTCTTTGCCAGGCAACGATCGGCGCCCGG
ACGAATACATTCTCGTGCGTCAAACGGGACAAGATGCTTTTACTGGTATTGCCAAA
GGCAACCTCGACCACATGCCCACCAAGGCGGAATTTAACGCGTGCTGCCGTCTCT
ACAGGGACGGAGCCGGTAATTACTATCCGCCACCTCTCGCGTTCGACAAGATTAG
CGTTCCAGCCCAACTGGAGGAAACATGGGGGATGATGGAGGCGAAGGAACGTAAC
AAACTACGGTTTCAGTACAAGTTGGACGTATGGAATCATGCGCACGCTGATATGGG
GATCACTGGCACAGAGATCT -3’ (underlined: 48 bp GFP_{11}-coding sequence; bold: the CCT codon of Proline39; double underlined: *Spe*I restriction site; italics: *Nde*I restriction site; dots: *Bgl*II restriction site). To insert the phiLOV2.1 coding sequence adjacent to the codon for proline-39, a similar DNA fragment was synthesized in which the GFP_{11} coding sequence was replaced by the 339 bp phiLOV2.1 coding sequence:

5’- ATGATAGAGAAGAGTTTCGTCATCACTGATCCTAGGCTTCCCGACTATCCCATTA
TCTTTGCATCAGACGGCTTTCTTGAATTGACAGAGTATTCGCGCGAGGAAATAATG
GGGAGAAATGCCCGGTTTCTTCAGGGGCCAGAGACAGATCAAGCGACTGTCCAGA
AGATAAGGGACGCAATTAGAGATCAGAGGGAGACTACTGTGCAGTTGATAAACTAC
ACTAAAAGCGGAAAGAAATTCTGGAACTTACTCCACCTGCAACCTGTGCGTGATCG
GAAGGGAGGGCTTCAATACTTCATCGGTGTGCAGCTCGTTGGAAGTGATCATGTAC
CCTAA -3’. To obtain full length *viE2* internally tagged with GFP_{11} or phiLOV2.1 the synthetic DNAs were used to replace the *Spe*I - *Bgl*II fragment with the 5’-end of *virE2* of pUG36YFP::VirE2 to generate pUG36YFP::39GFP_{11}-VirE2 and pUG36YFP::39phiLOV2.1-VirE2, respectively. For expression in yeast an *Xba*I–*Xho*I fragment containing tagged *virE2*, was ligated into pUG34 digested with *Xba*I and *Xho*I yielding pUG34::39GFP_{11}-VirE2 and pUG34::39phiLOV2.1-VirE2. For expression in *Agrobacterium* pSDM3163::39GFP_{11}[VirE2] and pSDM3163::39phiLOv2.1[VirE2] (pBBR6-derived plasmids) were constructed by replacing the *Nde*I – *Hind*III fragment with N-terminally tagged *virE2* of pSDM3163::GFP_{11}[VirE2] (Sakalis *et al* ., 2014) by the

*Nde*I-*Hind*III fragment of pUG34-39GFP$_{11}$[VirE2] and pUG34-39phiLOV2.1[VirE2]. The constructed plasmids were checked by sequencing using primers VirE2-seq-FW, VirE2-seq-Rev and VirE2-seq-int (Table S4).

For expression of phiLOV2.1-tagged effector proteins in *Agrobacterium*, plasmid pBBR6 was used. To construct pBBR6[phiLOV2.1-VirD2], first a DNA fragment with the *virD* promoter was amplified from pSDM3076 by PCR using the primers *Eco*RI-pVirD2-Fw and *Pst*I-pVirD2-Rev. This fragment was ligated into pBBR6 after digestion with *Eco*RI and *Pst*I. Subsequently, a DNA fragment with phiLOV2.1 was amplified from pUG36phiLOV2.1 using the primers *Pst*I-phiLOV2.1-Fw and *Spe*I-phiLOV2.1ΔTAA –Rev and ligated into pBBR6-pVirD2 digested with *PstI* and *SpeI*. *Spe*I-VirD2-Fw and *Xba*I-VirD2-Rev were used to get the fragment *Spe*I-VirD2-*Xba*I using pSDM3149 as a PCR template, which was then cloned in pBBR6-phiLOV2.1 digested with *Spe*I and *Xba*I. pBBR6[phiLOV2.1-VirD5] was constructed by ligation of the fragment *Eco*RI-*virD* promoter-*Pst*I, obtained by PCR from pSDM3759 with the primers *Eco*RI-pVirD-Fw and *Pst*I-pVirD-Rev, into pBBR6 using *Eco*RI and *Pst*I. The primers *Pst*I-phiLOV2.1-Fw and *Xma*I-phiLOV2.1-Rev were used to generate *Pst*I-phiLOV2.1-*Xma*I from pUG36 phiLOV2.1 and followed by ligation into pBBR6-p*virD* plasmid digested by *PstI* and *XmaI*. The primers, *Xma*I-VirD5-Fw and *Xba*I-VirD5-Rev were used to generate *Xma*I-VirD5-*Xba*I from pSDM3759. Subsequently, *XmaI*-VirD5-*XbaI* fragment was ligated into pBBR6 containing the *virD* promoter and phiLOv2.1 using *XmaI* and *Xba*I. The plasmids pBBR6[phiLOV2.1-VirE2] and pBBR6[phiLOV2.1-VirE3] were made by ligating first the *Eco*RI-*virE* promoter-*Pst*I fragment into the vector pBBR6. This promoter was obtained by PCR using *Eco*RI-pVirE-Fw and *Pst*I-pVirE-Rev on pSDM3163::39phiLOv2.1[VirE2]. A *Pst*I-*Bam*HI fragment containing phiLOV2.1ΔTAA was obtained by PCR from pUG36phiLOV2.1 with the primers *PstI*-phiLOV2.1-Fw and *Bam*HI-phiLOV2.1ΔTAA-Rev and subsequently ligated into pBBR6-VirE promoter backbone digested with *PstI* and *BamHI* to generate pBBR6-pVirE-PhiLOv2.1. To create pBBR6[phiLOV2.1-VirE2], the *Bam*HI-VirE2-*Xba*I fragment, obtained with *Bam*HI-VirE2-Fw and *Xba*I-VirE2-Rev from pJET[VirE2], was ligated into pBBR6[pVirE- phiLOV2.1] digested with *Bam*HI and *Xba*I. pBBR6[phiLOV2.1-VirE3] was constructed in the same way, using pUG36[GFP$_{11}$-VirE3]

as a template for the PCR, using primers *Bam*HI-VirE3-Fw and *Xba*I-VirE3-Rev. To express phiLOV2.1-tagged VirE2 under control of *35S* promoter in protoplasts, we constructed pART7[39phiLOV2.1-VirE2]. To this end, first phiLOV2.1-tagged *virE2*, was amplified by PCR on pBBR6[39phiLOV2.1-VirE2] using the primers *KpnI*-39phiLOVE2-Fw and *XbaI*-39phiLOVE2-Rev. Then, pART7[39phiLOV2.1-VirE2] was created by ligation of *XbaI-KpnI* 39phiLOV2.1-VirE2 fragment into *XbaI* and *KpnI* digested pART7.

ACKNOWLEDGEMENTS

We would like to thank Lan-Ying Lee and Stanton Gelvin (Purdue University) for providing the *A. thaliana* Col-0 mRFP-NLS seeds (At2051), John M. Christie (University of Glasgow, UK) for the plasmid containing the phiLOV2.1 coding sequence, and Gerda Lamers (our institute) for her help with microscopy. We acknowledge Philippe Sakalis for construction of plasmids allowing GFP_{11}-tagged effector proteins and images used in Figure 3 (I and K). This study is partly supported by a grant from the Royal Academy of Sciences of The Netherlands.

SUPPORTING INFORMATION

Figure S1. Nuclear localization of ectopically expressed GFP_{11}- and phiLOV2.1-tagged VirD2 and VirD5 in yeast.

Figure S2. Control microscopy for the detection of phiLOV2.1 in yeast.

Figure S3. Biological activity assessments.

Figure S4. Confocal microscopy of *A. thaliana* root explants co-cultivated for 48 hrs with *Agrobacterium* strain LBA2573(39phiLOV2.1-VirE2.

Figure S5. Control microscopy for the detection of phiLOV2.1 in plants.

Figure S6. Schematic overview of the putative endocytic motifs.

Movie S1. Movement of translocated 39GFP_{11}-VirE2 inside *N. tabacum* expressing GFP_{1-10} cells.

Table S1. Yeast strains used in this study

Table S2. *Agrobacterium* strains used in this study

Table S3. Plasmids used in this study

Table S4. Primers used in this study

COMPETING FINANCIAL INTERESTS

The authors declare no competing financial interests.

REFERENCES

Abràmoff, M. D., Magalhães, P. J. and Ram, S. J. (2004). Image processing with imageJ. *Biophotonics Int.* 11, 36–41.

Albright, L.M., Yanofsky, M.F., Leroux, B., Ma, D.Q. and Nester, E.W. (1987). Processing of the T-DNA of *Agrobacterium tumefaciens* generates border nicks and linear, single-stranded T-DNA. *J. Bacteriol.* 169, 1046–1055.

Buckley,A.M., Petersen,J., Roe,A.J., Douce,G.R. and Christie,J.M. (2015) LOV-based reporters for fluorescence imaging. Curr. Opin. Chem. Biol. 27, 39–45.

Christie, P.J., Atmakuri, K., Krishnamoorthy, V., Jakubowski, S. and Cascales, E. (2005). Biogenesis, Architecture, and Function of Bacterial Type Iv Secretion Systems. *Annu. Rev. Microbiol.* 59, 451–485.

Christie, J.M., Gawthorne, J.A., Young, G., Fraser, N.J. and Roe, A.J. (2012a). LOV to BLUF: Flavoprotein contributions to the optogenetic toolkit. *Mol. Plant,* 5, 533–544.

Christie, J.M., Hitomi, K., Arvai, A.S., Hartfield, K.A., Mettlen, M., Pratt, A.J., Tainer, J.A. and Getzoff, E.D. (2012b). Structural tuning of the fluorescent protein iLOV for improved photostability. *J. Biol. Chem.* 287, 22295–22304.

Citovsky, V., Wong, ML. and Zambryski, P. (1989). Cooperative interaction of Agrobacterium VirE2 protein with single-stranded DNA: Implications for the T-DNA transfer process. *Proc. Natl. Acad. Sci. USA.* 86,1193–1197.

Citovsky, V., Zupan, J., Warnick, D. and Zambryski, P. (1992). Nuclear localization of *Agrobacterium* VirE2 protein in plant cells. *Science,* 256, 1802–5.

Citovsky, V., D. Warnick. and P. Zambryski. (1994). Nuclear import of Agrobacterium VirD2 and VirE2 proteins in maize and tobacco. *Proc. Natl. Acad. Sci. USA*, 91,3210–3214.

De Cleene, M. and De Ley, J. (1976). The host range of crown gall. *Bot. Rev.* 42, 389–466.

den Dulk-Ras, A. and Hooykaas, P.J.J. (1995). Electroporation of *Agrobacterium tumefaciens*. *Methods Mol. Biol.* 55, 63–72.

Djamei, A., Pitzschke A., Nakagami, H., Rajh, I. and Hirt, H. (2007). Trojan horse strategy in *Agrobacterium* transformation: abusing MAPK defense signaling. *Science*, 318, 453–456.

García-Rodríguez, F.M., Schrammeijer, B. and Hooykaas, P.J.J. (2006). The *Agrobacterium* VirE3 effector protein: a potential plant transcriptional activator. *Nucleic Acids Res.* 34, 6496–6504.

García-Cano, E., Hak, H., Magori, S., Lazarowitz, S. and Citovsky, V. (2017). The Agrobacterium F-box protein effector VirF destabilizes the Arabidopsis GLABROUS1

enhancer/binding protein-like transcription factor VFP4, a transcriptional activator of defense response genes. *Mol Plant Microbe Interact.* doi: 10.1094/MPMI-07-17-0188-FI.

Gawthorne, J.A., Audry, L., McQuitty, C., Dean, P., Christie, J.M., Enninga, J. and Roe, A.J. (2016). Visualizing the translocation and localization of bacterial type III effector proteins by using a genetically encoded reporter system. *Appl. Environ. Microbiol.* 82, 2700–2708.

Gietl, C., Koukolfkova-Nicola, Z. and Hohn, B. (1987). Mobilization of T-DNA from *Agrobacterium* to plant cells involves a protein that binds single-stranded DNA. *Cell Biol.* 84, 9006–9010.

Gietz, R. D., Schiestl, R. H., Willems, A. R. and Woods, R. A. (1995). Studies on the transformation of intact yeast-cells by the LiAc/ssDNA/PEG procedure . *Yeast*, *11*(N4), 355–360.

Herrera-Estrella, A.,Van Montagu, M. and Wang, K.(1990).A bacterial peptide acting as a plant nuclear targeting signal: the amino-terminal portion of *Agrobacterium* VirD2 protein directs a β-galactosidase fusion protein in to tobacco nuclei. *Proc.Natl.Acad.Sci.USA,* 87, 9534–9537.

Hooykaas, P. J. J., Hofker, M., Dulk-Ras, A. den. **and Schilperoort, R. A.**1(984). A comparison of virulence determinants in an octopine Ti plasmid, a nopaline Ti plasmid, and an Ri plasmid by complementation analysis of *Agrobacterium tumefaciens* mutants. *Plasmid,* 11**,** 195–205.

Howard, E.A., Zupan, J.R., Citovsky, V. and Zambryski, P.C. (1992). The VirD2 protein of *A. tumefaciens* contains a C-terminal bipartite nuclear localization signal: Implications for nuclear uptake of DNA in plant cells. *Cell*, 68, 109–118.

Huala, E., Oeller, P.W., Liscum, E., Han, I.S., Larsen, E. and Briggs, W.R. (1997). *Arabidopsis* NPH1: a protein kinase with a putative redox-sensing domain. *Science*, 278, 2120–2123.

Larebeke, N. Van., Engler, G., Holsters, M., Elsacker, S. Van Den, Zaenen, I., Schilperoort, R.A. and Schell, J. (1974). Large plasmid in *Agrobacterium tumefaciens* essential for crown gall-inducing ability. *Nature*, 252, 169–170.

Lee, Y.W., Jin, S., Sim, W.S. and Nester, E.W. (1996). The sensing of plant signal molecules by *Agrobacterium*: Genetic evidence for direct recognition of phenolic inducers by the VirA protein. *Gene*, 179, 83–88.

Li, X., Yang, Q., Tu, H., Lim, Z. and Pan, S. Q. (2014). Direct visualization of Agrobacterium-delivered VirE2 in recipient cells. *Plant J. 77*(3), 487–495.

Li, X. and Pan, S.Q. (2017). *Agrobacterium* delivers VirE2 protein into host cells via clathrin-mediated endocytosis. *Sci. Adv.* 3.

Magori, S. and Citovsky, V. (2011). Hijacking of the host SCF ubiquitin ligase machinery by plant pathogens. *Front. Plant. Sci.* 2, 87.

Melchers, L.S., Maroney, M.J., Dulk-Ras, A.den.,Thompson,D.V., Vuuren, H.A.J., Schilperoort, R.A. and Hooykaas, P.J.J. (1990). Octopine and nopaline strains of Agrobacterium tumefaciens differ in virulence; molecular characterization of the virF locus. *Plant Mol Biol.* 14, 249–259.

Mysore, K.S., Bassuner, B., Deng, X. B., Darbinian, N.S., Motchoulski, A., Ream,W. and Gelvin, S. B.(1998).Role of the *Agrobacterium tumefaciens* VirD2 protein in T-DNA transfer and integration. *Mol. Plant. Microbe. Interact.* 11, 668–683.

Nester, E.W., Watson, B., Currier, T.C., Gordon, M.P. and Chilton, M. (1975). Plasmid required for virulence of *Agrobacterium* Plasmid Required for Virulence of *Agrobacterium tumefaciens*. *J. Bacteriol.* 123, 255.

Nester, E.W., Gordon, M.P., Amasino, R.M. and Yanofsky, M.F. (1984). Crown gall: A molecular and physiological analysis*. Annu Rev Plant Physiol*. 35, 387–413.

Niu, X., Zhou, M., Henkel, C. V., Heusden, G.P.H. Van. and Hooykaas, P.J.J. (2015). The *Agrobacterium tumefaciens* virulence protein VirE3 is a transcriptional activator of the F-box gene VBF. *Plant J.* 84, 914–924.

Pansegrau, W., Schoumacher, F., Hohn, B. and Lanka, E. (1993). Site-specific cleavage and joining of single-stranded DNA by VirD2 protein of *Agrobacterium tumefaciens* Ti plasmids: analogy to bacterial conjugation. *Proc. Natl. Acad. Sci. USA*, 90, 11538–42.

Park, E., Lee, H.-Y., Woo, J., Choi, D. and Dinesh-Kumar, S.P. (2017). Spatiotemporal monitoring of Pseudomonas syringae effectors via type III secretion using split fluorescent protein fragments. *Plant Cell.,* 29, 1571–1584.

Rossi, L., Hohn, B. and Tinland, B. (1993).The VirD2 protein of *Agrobacterium tumefaciens* carries nuclear localization signals important for transfer of T-DNA to plant. *Mol.Gen.Genet.,* 239, 345–353.

Rossi, L., Hohn, B. and Tinland, B. (1996). Integration of complete transferred DNA units is dependent on the activity of virulence E2 protein of *Agrobacterium tumefaciens*. *Proc. Natl. Acad. Sci. USA*, 93, 126–30.

Sakalis, P.A. (2013). Visualizing virulence proteins and their translocation into the host during *Agrobacterium*-mediated transformation. PhD.-thesis. Leiden University.

Sakalis, P.A., Heusden, G.P.H. van. and Hooykaas, P.J.J. (2014). Visualization of VirE2 protein translocation by the *Agrobacterium* type IV secretion system into host cells. *Microbiologyopen,* 3, 104–117.

Salman, H., Abu-Arish, A., Oliel, S., Loyter, A., Klafter, J., Granel, R. and Elbaum, M. (2005). Nuclear localization signal peptides induce molecular delivery along microtubules. *Biophys J*. 89,2134-2145.

Shi, Y., Lee, L.-Y. and Gelvin, S. B. (2014). Is VIP1 important for *Agrobacterium*-mediated transformation? *Plant J.* 79, 848–860.

Schirawski, J., Planchais, S. and Haenni, A.L. (2000) An improved protocol for the preparation of protoplasts from an established Arabidopsis thaliana cell suspension culture and infection with RNA of turnip yellow mosaic tymovirus: a simple and reliable method. *J. Virol. Methods*. 86, 85–94.

Schrammeijer, B., Risseeuw, E., Pansegrau, W., Regensburg-Tuink, A.J.G., Crosby, W.L. and Hooykaas, P.J.J. (2001). Interaction of the virulence protein VirF of *Agrobacterium tumefaciens* with plant homologs of the yeast Skp1 protein. *Curr. Biol*. 11. 258–262.

Shurvinton, C.E., Hodges, L. and Ream, W.(1992).A nuclear localization signal and the C- terminal omega sequence in the *Agrobacterium tumefaciens* VirD2 endonuclease are important for tumor formation. *Proc. Natl. Acad. Sci. USA,* 89, 11837–11841.

Stachel, S.E. and Nester, E.W. (1986). The genetic and transcriptional organization of the vir region of the A6 Ti plasmid of *Agrobacterium tumefaciens*. *EMBO J.* 5, 1445–54.

Tinland, B., Koukolikova-Nicola, Z., Hall, M.N. and Hohn, B. (1992). The T-DNA-linked VirD2protein contains two distinct functional nuclear localization signals. *Proc. Natl. Acad. Sci.USA,* 89, 7442–7446.

Tinland, B., Hohn, B. and Puchta, H. (1994). *Agrobacterium tumefaciens* transfers single-stranded transferred DNA (T-DNA) into the plant cell nucleus. *Proc. Natl. Acad. Sci. USA*, 91, 8000–4.

Tzfira, T., Vaidya, M. and Citovsky, V. (2001). VIP1, an *Arabidopsis* protein that interacts with *Agrobacterium* VirE2, is involved in VirE2 nuclear import and *Agrobacterium* infectivity. *EMBO J.* 20, 3596–3607.

Tzfira, T., Vaidya, M. and Citovsky, V. (2004). Involvement of targeted proteolysis in plant genetic transformation by *Agrobacterium*. *Nature*, 431, 87–92.

van Engelenburg, S. B. and Palmer, A. E. (2010). Imaging type-III secretion reveals dynamics and spatial segregation of Salmonella effectors. *Nat. Methods,* 7, 325–330.

Vergunst, A. (1998). Root transformation by *Agrobacterium tumefaciens*. In J. M. Martinez-Zapater and J. Salinas, eds. *Methods in Molecular Biology*, 227–44.

Vergunst, B., Dulk-Ras, A. Den., Vlaam, C.M.T., Regensburg-Tuink, T.J.G. and Hooykaas, P.J.J., (2000). VirB/D4 dependent protein translocation from *Agrobacterium* into plant cells. *Science,* 290, 979–981.

Vergunst, A.C., Lier, M.C.M., Dulk-Ras, A. Den., Grosse Stüve, T.A., Ouwehand, A. and Hooykaas, P.J.J. (2005). Positive charge is an important feature of the C-terminal transport signal of the VirB/D4-translocated proteins of *Agrobacterium*. *Proc. Natl. Acad. Sci. United States Am.* 102, 832–837.

Vogel, A.M. and Das, A.(1992).Mutational analysis of *Agrobacterium tumefaciens* virD2:tyrosine29is essential for endonuclease activity. *J. Bacteriol.* 174, 303–308.

Wang, Y., Peng, W., Zhou, X., Huang, F., Shao, L. and Luo, M. (2014). The putative *Agrobacterium* transcriptional activator-like virulence protein VirD5 may target T-complex to prevent the degradation of coat proteins in the plant cell nucleus. *New Phytol.* 203, 1266–1281.

Wang,Y., Zhang, S., Huang, F., Zhou, X., Chen, Z., Peng, W. and Luo, M. (2018). VirD5 is required for efficient Agrobacterium infection and interacts with Arabidopsis VIP2. *New Phytol*. 217, 726–738.

Wolterink-van Loo, S., Escamilla Ayala, A. A., Hooykaas, P. J.J. and van Heusden, G. P. H. (2015). Interaction of the *Agrobacterium tumefaciens* virulence protein VirD2 with histones. Microbiology, 161:401–410.

Yang, Q., Li, X., Tu, H. and Pan, S.Q. (2017). *Agrobacterium* -delivered virulence protein VirE2 is trafficked inside host cells via a myosin XI-K–powered ER/actin network. *Proc. Natl. Acad. Sci*.114, 2982–2987.

Zaltsman, A., Krichevsky, A., Loyter, A. and Citovsky, V. (2010). *Agrobacterium* Induces Expression of a Host F-Box Protein Required for Tumorigenicity. *Cell Host Microbe*, 7, 197–209.

Zhang, X., Heusden, G.P.H. van. and Hooykaas, P.J.J.(2017).Virulence protein VirD5 of Agrobacterium tumefaciens binds to kinetochores in host cells via an interaction with Spt4. *Proc. Natl. Acad. Sci.USA,38,* 10238–10243.

Zhou, X. R. and P. J. Christie. (1999). Mutagenesis of the Agrobacterium VirE2 single-stranded DNA-binding protein identifies regions required for self-association and interaction with VirE1 and a permissive site for hybrid protein construction. *J. Bacteriol.* 181, 4342–4352.

Zhu, J., Oger, P.M., Schrammeijer, B., Hooykaas, P.J.J., Farrand, S.K. and Winans, S.C. (2000) The bases of crown gall tumorigenesis. J Bacteriol. 182, 3885– 3895.

Ziemienowicz, A., Merkle, T., Schoumacher, F., Hohn, B. and Rossi, L. (2001). Import of *Agrobacterium* T-DNA into plant nuclei: two distinct functions of VirD2 and VirE2 proteins. *Plant Cell,* 2001., 13, 369–83.

Zonneveld, B.J.M. (1986). Cheap and simple yeast media. *J Microbiol Methods,4,287*–291.

FIGURE LEGENDS.

Figure 1. **Visualization of ectopically expressed phiLOV2.1- and GFP_{11}-tagged *Agrobacterium* effector proteins in yeast.** Upper panel, confocal microscopy of yeast strain BY4741 transformed with pUG36-39phiLOV2.1-VirE2 (A), with pUG36-phiLOV2.1-VirE2 (N-terminally tagged) (B), with pUG36-phiLOV2.1-VirD2 (C), with pUG36-phiLOV2.1-VirF (D), with pUG36-phiLOV2.1-VirD5 (E), or with pUG36-phiLOV2.1-VirE3 (F). Lower panel, confocal microscopy of yeast strain 426::GFP_{1-10} transformed with pUG34[39GFP_{11}-VirE2] (G), with pUG34GFP_{11}[VirE2] (N-terminally tagged) (H), with pUG34GFP_{11}[VirD2] (I), or with pUG34GFP_{11}[VirD5] (K). Scale bars: 5 µm.

Figure 2. **Analysis of 39phiLOV2.1-VirE2 expression in *Agrobacterium* by fluorescent microscopy.** A, LBA2572(3163-39phiLOV2.1-VirE2) (containing T-DNA) induced with acetosyringone for 6 hrs. B, LBA2573(3163-39phiLOV2.1-VirE2) (lacking T-DNA) induced with acetosyringone for 6 hrs. C, LBA2572(3163-39phiLOV2.1-VirE2) (containing T-DNA) induced with acetosyringone for 24 hrs. D, LBA2573(3163-39phiLOV2.1-VirE2) (lacking T-DNA) induced with acetosyringone for 24 hrs. AS, acetosyringone. Scale bars: 2µm.

Figure 3. **Visualization of translocated phiLOV2.1- and GFP_{11}-tagged effector proteins in yeast by confocal microscopy**. Confocal microscopy of BY4741 (A-F) and 426::GFP_{1-10} (G-K) yeast cells after co-cultivation with *Agrobacterium* strains LBA2573(3163-39phiLOV2.1-VirE2)(A), with LBA2573(pBBR6-phiLOV2.1-VirE2) (B), with LBA2556(pBBR6-phiLOV2.1-VirD2) (C), with LBA2561(pBBR6-phiLOV2.1-VirF) (D), with LBA3551(pBBR6-phiLOV2.1-VirD5) (E), with LBA2565(pBBR6-phiLOV2.1-VirE3) (F), with LBA2573(3163-39GFP_{11}-VirE2) (G), with LBA2573(3163-GFP_{11}-VirE2) (H), with LBA2556(3163GFP_{11}-D2) (I), or with LBA3551(3076GFP_{11}-D5) (K). Scale bars: 5 µm.

Figure 4. **Translocation of phiLOV2.1-tagged effector proteins from *Agrobacterium* to *A. thaliana* Col-0 (NLS-RFP) roots.** Roots were agroinfiltrated with Agrobacterium strains LBA2573(3163-39phiLOV2.1-VirE2) (A), with LBA2569(3163GFP_{11}-D2) (B), with

LBA3550(3076GFP$_{11}$-D5) (C), or with LBA2560(3163GFP$_{11}$-F) (D). Images were captured 15 hours (A), 42 hours (B), 44 hours (C) and 23 hours (D) after agroinfiltration. White arrows indicate perinuclear and nuclear signals. Scale bars: 15 µm.

Figure 5. **Visualization of 39phiLOV2.1-VirE2] translocation from *Agrobacterium* to *N. tabacum* leaves.** Leaves of *N. tabacum* SR1 wild type plants were agroinfiltrated with LBA2572(3163-39phiLOV2.1-VirE2) (containing T-DNA)(A and C) or with LBA2573(3163-39phiLOV2.1-VirE2) (lacking T-DNA)(B and D) and images were captured after 21 hrs. Both cytoplasmic localizations (A and B) and membrane localizations (C and D) of translocated 39phiLOV2.1-VirE2 were observed. CF, chlorophyll fluorescence. Scale bars: 30µm.

Figure 6. **Translocated phiLOV2.1-tagged VirE3, -VirD2, -VirF and -VirD5 localized near the plasma membrane in *N. tabacum* SR1 leaves.** *N. tabacum* SR1 wild type plants were agroinfiltrated with LBA2564(pBBR6-phiLOV2.1-VirE3) (A), with LBA2569(pBBR6-phiLOV2.1-VirD2) (B), with LBA2560(3163GFP$_{11}$-F) (C) or with LBA3551(pBBR6-phiLOV2.1-VirD5) (D). Images were captured by confocal microscopy after 42 hrs. Red signals, chlorophyll fluorescence. Scale bars: 25µm.

Figure 7. **Effect of the microtubule-disturbing drugs benomyl and oryzalin on the localization of 39phiLOV2.1-VirE2 in yeast and *A. thaliana* protoplasts**. Upper panel, cells of yeast strain BY4741 harboring pUG36-39phiLOv2.1-VirE2 were exposed to the indicated amounts of benomyl or DMSO for 45 or 90 minutes and the localization of 39phiLOv2.1-VirE2 was analyzed by confocal microscopy. Scale bars: 5 µm. Lower panel, *A.thaliana* protoplasts harboring pART7[39phiLOV2.1-VirE2] were exposed to oryzalin or DMSO for 60 min and the localization of 39phiLOv2.1-VirE2 was analyzed by confocal microscopy. Scale bars: 25µm.

FIGURES

Figure 1.

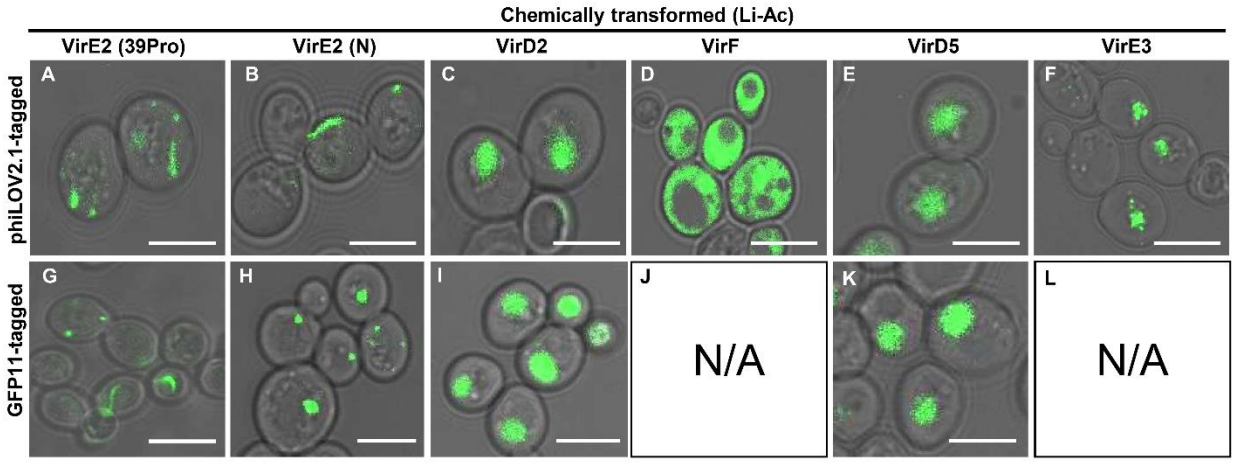

Figure 2.

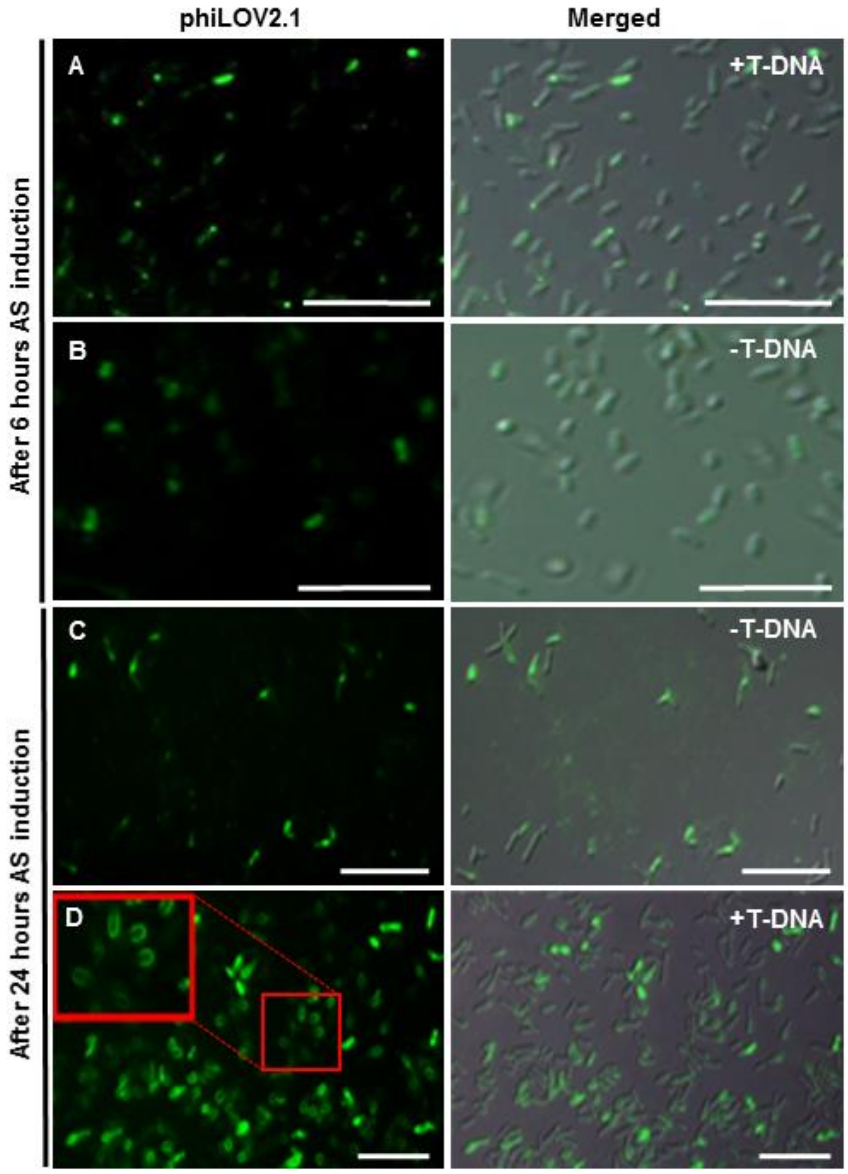
phiLOV2.1
Merged
A
+T-DNA
B
-T-DNA
C
-T-DNA
D
+T-DNA
After 6 hours AS induction
After 24 hours AS induction

Figure 3.

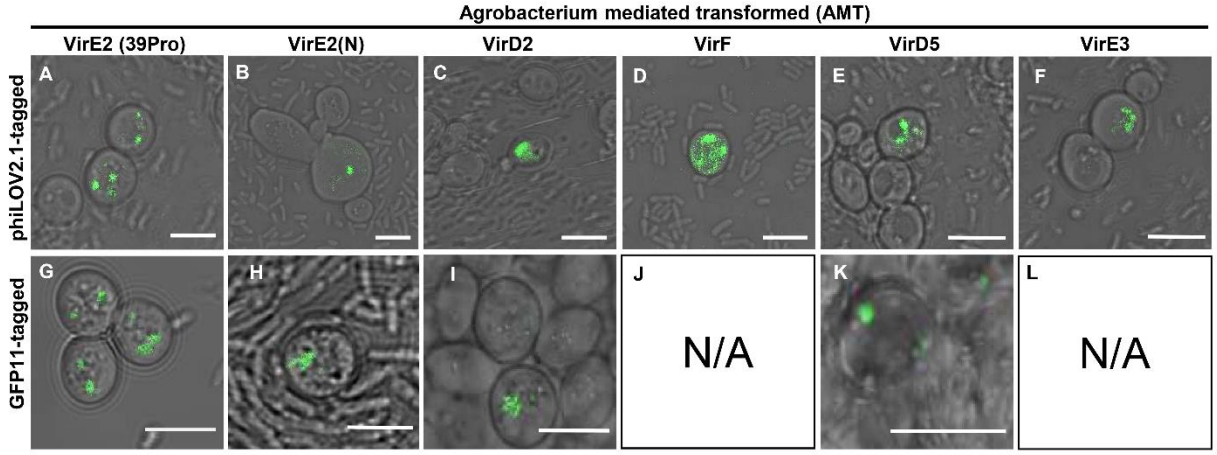
Agrobacterium mediated transformed (AMT)
VirE2 (39Pro)
VirE2(N)
VirD2
VirF
VirD5
VirE3
phiLOV2.1-tagged
GFP11-tagged
A
B
C
D
E
F
G
H
I
J
K
L
N/A
N/A

Figure 4.

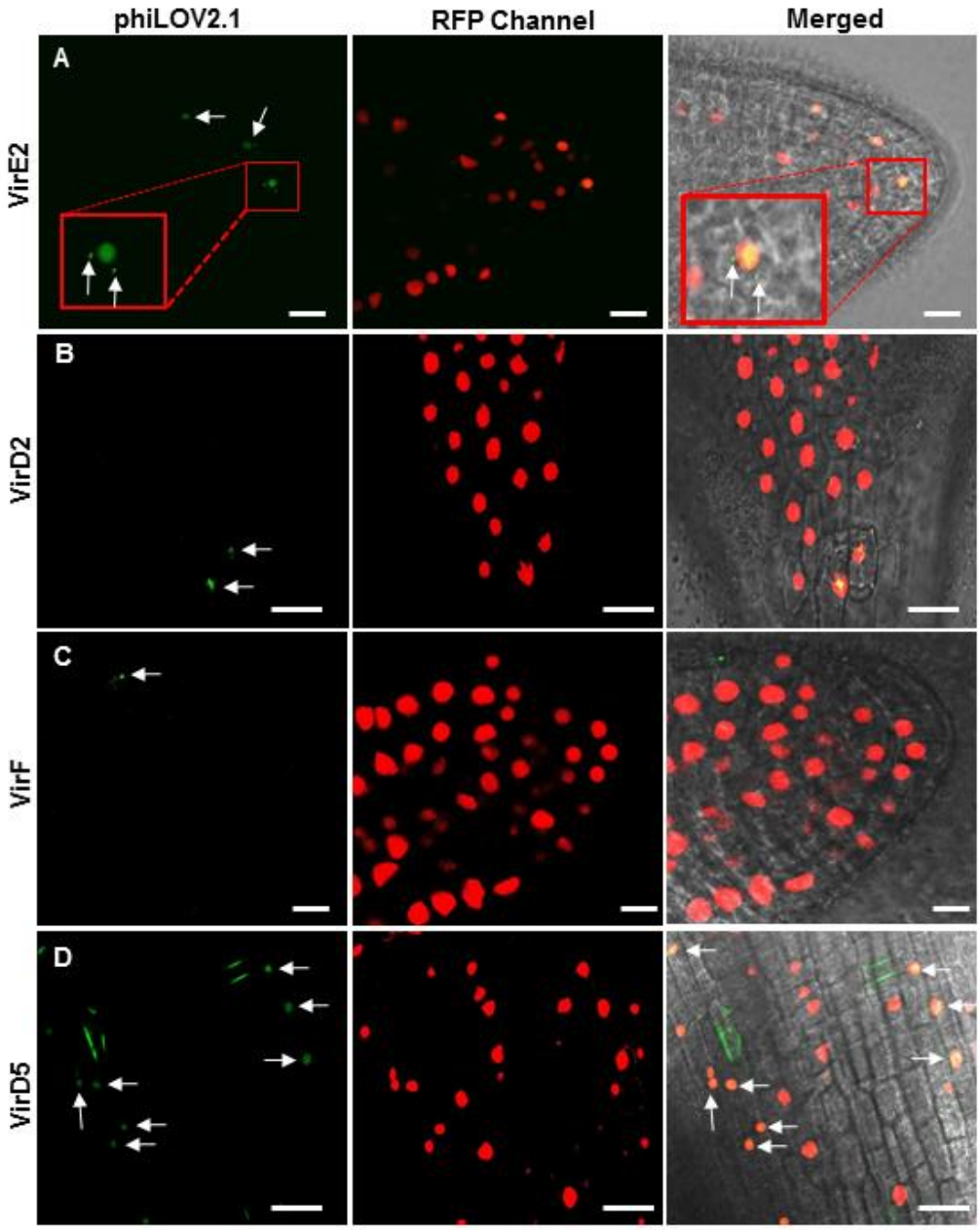

Figure 5.

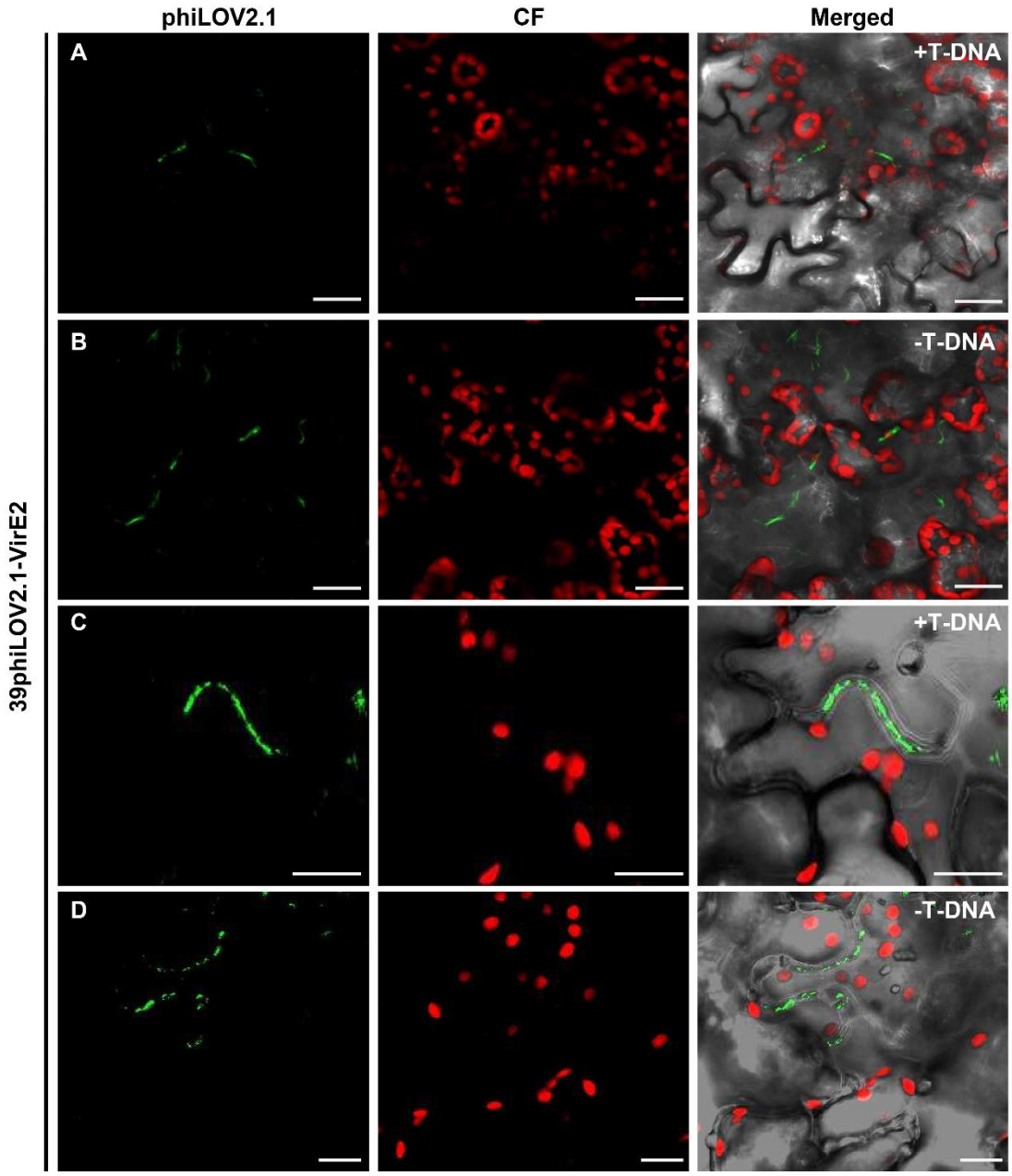
phiLOV2.1
CF
Merged
39phiLOV2.1-VirE2
A
+T-DNA
B
-T-DNA
C
+T-DNA
D
-T-DNA

Figure 6.

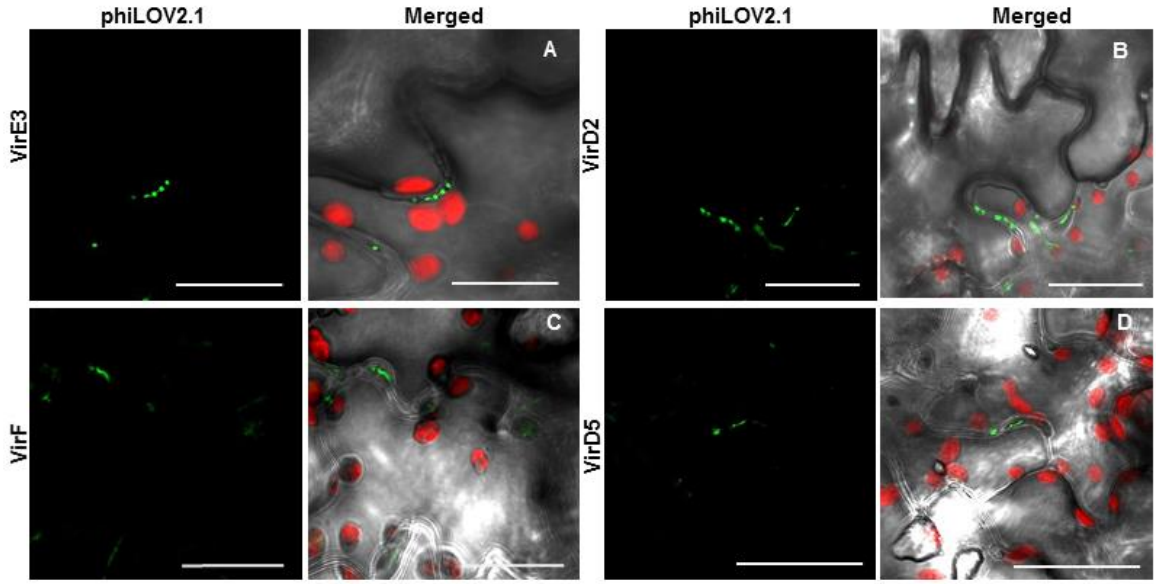
phiLOV2.1
Merged
phiLOV2.1
Merged
VirE3
VirD2
VirF
VirD5
A
B
C
D

Figure 7.

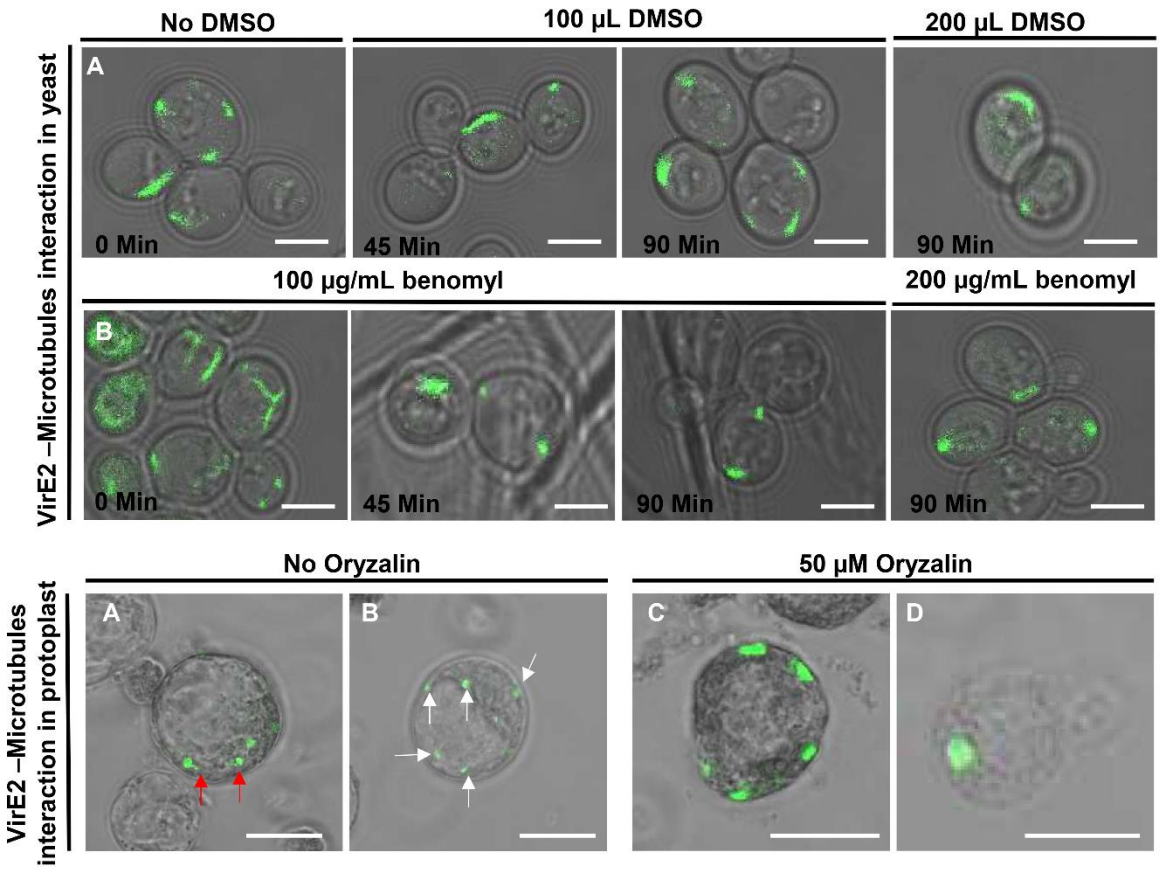
No DMSO
100 µL DMSO
200 µL DMSO
A
0 Min
45 Min
90 Min
90 Min
VirE2 –Microtubules interaction in yeast
100 µg/mL benomyl
200 µg/mL benomyl
B
0 Min
45 Min
90 Min
90 Min
No Oryzalin
50 µM Oryzalin
A
B
C
D
VirE2 –Microtubules interaction in protoplast